


## Focused ultrasound stimulation on meibomian glands for the treatment of evaporative dry eye

Gengxi Lu<sup>1,2</sup> , Sumanth Gollapudi<sup>1</sup>, Runze Li<sup>1,2</sup>, Margaret L Pfeiffer<sup>1</sup>, Preeya Mehta<sup>1</sup>, Laiming Jiang<sup>1,2</sup>, Sarah Hamm-Alvarez<sup>1,3</sup>, Mark Humayun<sup>1,2,4</sup>, Qifa Zhou<sup>1,2</sup> and Sandy X Zhang-Nunes<sup>1</sup>

<sup>1</sup>Roski Eye Institute, Dry Eye Center of Excellence, Keck School of Medicine, University of Southern California, Los Angeles, CA 90033, USA; <sup>2</sup>Department of Biomedical Engineering, University of Southern California, Los Angeles, CA 90089, USA; <sup>3</sup>Department of Pharmacology and Pharmaceutical Sciences, School of Pharmacy, University of Southern California, Los Angeles, CA 90033, USA; <sup>4</sup>USC Ginsburg Institute for Biomedical Therapeutics, Keck School of Medicine, University of Southern California, Los Angeles, CA 90033, USA  
Corresponding authors: Sandy X Zhang-Nunes. Email: Sandy.Zhang-Nunes@med.usc.edu; Qifa Zhou. Email: qifazhou@usc.edu

### Impact statement

Current technologies to treat meibomian gland dysfunction are limited. It is important to find a more advanced technology for the treatment. As a pilot study, this work used focused ultrasound as a treatment for meibomian gland dysfunction, as it is expected to have unique advantages over other modalities. This work could potentially lead to an in-office or home-use medical device to treat dry eye disease conveniently and safely.

### Abstract

Current treatments for meibomian gland dysfunction have several limitations, creating a necessity for other advanced treatment options. The purpose of this study is to determine the effectiveness of focused ultrasound stimulation for the treatment of dry eye disease caused by meibomian gland dysfunction. An *in vivo* study of nine Dutch Belted rabbits was conducted with focused ultrasound stimulation of the meibomian glands. A customized line-focused ultrasonic transducer was designed for treatment. Fluorescein imaging, Schirmer's test, and Lipiview II ocular interferometer were used to quantify outcomes from three aspects: safety, tear production, and lipid layer thickness. Both tear secretion and lipid

layer thickness improved following ultrasound treatment. Five to 10 min after the ultrasound treatment, the mean values of lipid layer thickness increased from  $55.33 \pm 11.15$  nm to  $95.67 \pm 22.77$  nm ( $p < 0.05$ ), while the mean values measured with the Schirmer's test increased from  $2.0 \pm 2.3$  to  $7.2 \pm 4.3$  ( $p < 0.05$ ). Positive effects lasted more than three weeks. Adverse events such as redness, swelling, and mild burn, occurred in two rabbits in preliminary experiments when the eyelids sustained a temperature higher than  $42^{\circ}\text{C}$ . No serious adverse events were found. The results suggest that ultrasound stimulation of meibomian glands can improve both tear production and lipid secretion. Ultimately, ultrasound stimulation has the potential to be an option for the treatment of evaporative dry eye disease caused by meibomian gland dysfunction.

**Keywords:** Dry eye disease, ultrasound stimulation, meibomian gland dysfunction, lipid layer thickness, Schirmer's test, FEM simulation

*Experimental Biology and Medicine* 2022; 247: 519–526. DOI: 10.1177/15353702211052035

### Introduction

Dry eye disease (DED) is one of the most common ophthalmic disorders. Population-based epidemiologic studies have estimated that the prevalence of DED ranges from 5% to 30%. Individuals 50 years or older are more likely to have DED. Some regions of the world, such as Asia, have a higher prevalence of DED than other regions.<sup>1–3</sup> Based on data from the largest U.S. studies of adults over 50 years of age, 3.23 million women and 1.68 million men in the United

States have mild-to-moderate or severe symptoms of DED.<sup>4,5</sup> As defined by the Dry Eye Workshop (2007), DED is a multifactorial disease of the tears and ocular surface that results in symptoms of discomfort, visual disturbance, and tear film instability with potential damage and inflammation of the ocular surface.<sup>6</sup> The final common denominators of DED are tear film hyperosmolarity and instability.<sup>3,7</sup>

DED has two main subtypes of tear film deficiency: aqueous tear deficiency and evaporative deficiency, which are secondary to changes in the function of the lacrimal gland and meibomian gland, respectively.<sup>8</sup> Meibomian gland dysfunction (MGD) is considered the most frequent cause of DED, accounting for more than 70% of DED cases.<sup>9</sup> The meibomian glands are located in the upper and lower eyelids and are responsible for excreting lipids onto the ocular surface, lubricating the ocular surface during blinking, and protecting against tear evaporation. Recent studies have shown that eyelid temperature significantly influences the secretions of the meibomian glands, also known as meibum. As eyelid temperature increases, secreted meibum shows a phase-transition phenomenon from a gel-like state to a fluid state. Higher temperatures reduce the viscosity of meibum and make it easier to distribute the fluid over the cornea. The phase-transition temperature of meibum is  $\sim 28^{\circ}\text{C}$ , as measured from healthy donors. However, in MGD patients, meibum has an altered lipid composition, leading to the phase-transition temperature increasing to higher than  $32^{\circ}\text{C}$ .<sup>10–13</sup> In this case, evaporative DED is induced by MGD because the generated gel-like meibum cannot transition into the fluid state to protect the aqueous part of the tear film from evaporation.

Given the importance of meibomian glands in DED pathogenesis, various devices that target these glands have been proposed. For example, intense pulsed light<sup>12</sup> and electrical stimulation<sup>14</sup> are used to stimulate the lacrimal or meibomian glands. Warming devices that heat the meibomian glands can also improve meibum secretion.<sup>15,16</sup> All of these devices have several advantages and limitations. For example, light and electrical stimulation are aimed to increase the tear and meibum generation but do not directly stimulate meibomian gland outflow. Also, several side effects, such as blistering and blepharitis, have been observed from these stimulations. Devices that function as warming goggles (Blephasteam<sup>®</sup>, Laboratoires Thea, Clermont-Ferrand, France) heat the meibomian glands to improve MGD, but cannot stimulate glandular

flow due to a lack of compressional effects that can enhance secretions.

Ultrasound is a safe technology that has been widely used for medical applications and is an emerging non-invasive treatment technique.<sup>17–20</sup> In this study, a novel focused ultrasound treatment modality was designed and applied to stimulate meibomian gland secretions in healthy rabbits. As a non-invasive treatment modality, ultrasound has both a heating and stimulating effect to improve meibomian gland secretions and MGD.

## Materials and methods

### Animals

The study utilized nine Dutch Belted rabbits (female, 6–7 months old, three for preliminary study and six for formal treatment). They underwent ultrasound treatment of their meibomian glands under anesthesia with a customized ultrasound transducer. All animals were managed in accordance with the Association for Research in Vision and Ophthalmology (ARVO) Statement for the Use of Animals in Ophthalmic and Vision Research. Procedures were approved by the Institutional Animal Care and Use Committee at the University of Southern California (IACUC Protocol 20838). All experiments were conducted during the daytime, and the experiment time on each rabbit was less than 1 h. The measurements were repeated three times per eye.

The experimental setup is shown in Figure 1. The rabbit was anesthetized with an intramuscular injection of ketamine and xylazine (35 mg/kg, 5 mg/kg). The treatment area was prepared by shaving the eyelids to remove any hair that could interfere with the ultrasound waves. A strip of Tegaderm (3M, MN, USA) was then applied over the eye to ensure the eyelids and nictitating membrane were closed during the treatment, as shown in Figure 1(d). A needle-type thermocouple, used to measure temperature, was positioned by inserting the lead into the Tegaderm over

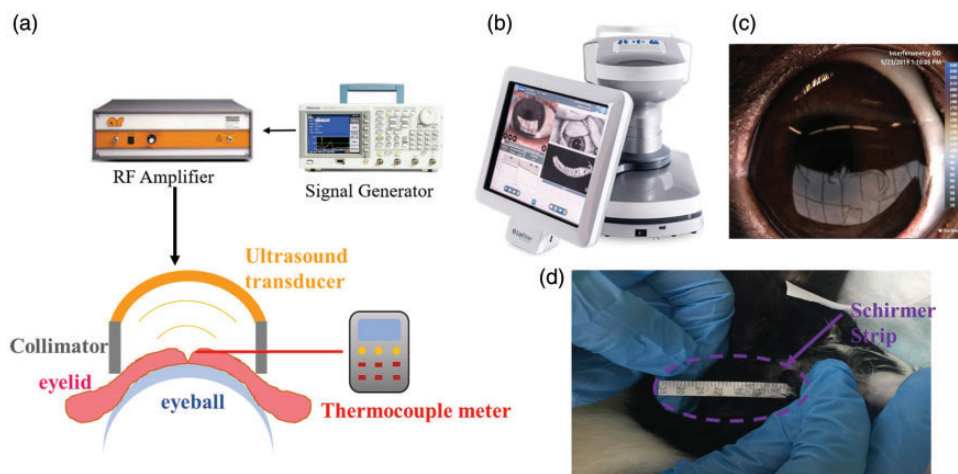


**Figure 1.** (a) Schematic diagram of the ultrasound treatment system. Monochromatic signals are generated and amplified by the waveform generator and amplifier. It drives the line-focus ultrasound transducer to treat the meibomian glands. The transducer is moved gently to cover upper and lower eyelids, approximately 2 s per sweep (the traversal from upper to lower eyelid then vice versa). A photo of the LipiView<sup>®</sup> II and a snapshot of its acquisition procedure are shown in (b) and (c). (d) A photo of conducting Schirmer's test on an anesthetized rabbit. (A color version of this figure is available in the online journal.)

the eyelid. The goal was to ensure that the eyelid temperature could be measured throughout the treatment. Ultrasound gel was then applied within the ultrasound transducer and on the Tegaderm in an area over the eyelids and thermocouple lead. The transducer was placed over the area with gel, and any gaps between the ultrasound transducer and the target area over the eye were filled in. Before application, ultrasound gel was heated using a water bath to 35°C to ensure that the gel did not cool the eyelid.

### Ultrasound transducer and parameters

A diagram of the ultrasound system is shown in Figure 1 (a). A customized, handheld transducer was used in this study. The transducer had a width of 24 mm, a length of 30 mm, and was line focused with a focal depth of 15 mm. For easier manipulation, a 3D-printed spacer was attached to the transducer's surface. The spacer was 1 mm shorter than the focal length to ensure that the focal line would be on the surface of the target tissue, as shown in Figure 2(b). The spacer was then filled with ultrasound gel as acoustic coupling. The transducer was scanned on the eyelids using a slow sweeping movement to cover the vertical heights of both the upper and lower eyelids (approximately 2 s going

from upper to lower eyelid, and 2 s going from lower to upper eyelid, and so on). A waveform generator (AFG3101, Tektronix, OR, USA) was used to drive the transducer, and the waveform generator was connected to an amplifier (100A250A, AMPLIFIER RESEARCH, PA, USA) with a gain of 50 dB.

Before the *in vivo* experiments, gelatin phantom experiments were conducted to quantify the heating ability of generated ultrasound and to determine the duty cycle and input voltage of the ultrasound. Parameters were chosen with the purpose of applying a gradual and stable temperature increase to the eyelids. The free-field ultrasound field was measured by the hydrophone (HGL-0400, ONDA, CA, USA) in a large water tank. To better illustrate the acoustic field and to confirm the ultrasound-induced temperature increase, an acoustic-bioheat simulation was conducted using finite-element analysis software. (COMSOL 5.3a, COMSOL Inc., MA, USA)

### In vivo ultrasound parameter optimization

Three healthy Dutch belted rabbits were initially used to test the ultrasound's safety and to optimize treatment parameters. The goal of these preliminary studies was to determine the appropriate timing of treatment as well as

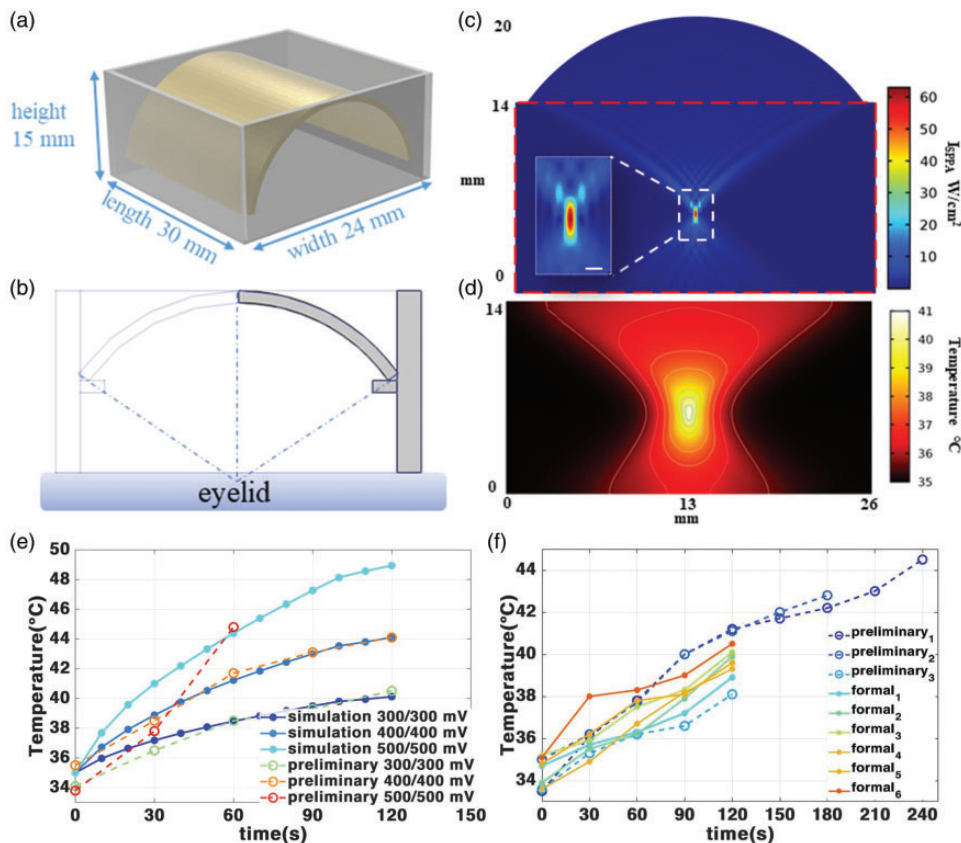


**Figure 2.** (a) The demonstration of the transducer and 3D-printed spacer. (b) The cross-sectional view of the transducer and spacer design. The spacer ensured that the focal area was located on the surface of the eyelid. (c) Simulated ultrasound field distribution showing the ultrasonic focal area; White bar: 0.4 mm. (d) Simulated temperature distribution caused by ultrasound heating effect. (Input voltage 300 mV, cycle number 300, heating time = 120 s.) (e) Ultrasound-induced temperature increase in simulation and preliminary experiments using different combinations of cycle number and input voltage (300/300 mV, 400/400 mV, 500/500 mV). (f) Ultrasound-induced temperature increase in preliminary experiments and formal experiments with 300 cycle number and 300 mV input voltage. Three sets of hollow circles with dotted lines indicate the temperature increase in the preliminary experiments. Six sets of solid circles and solid lines are from the formal experiments. Eyelid temperatures are controlled to be no higher than 41°C in formal experiments. (A color version of this figure is available in the online journal.)

the ultrasound parameters that would produce an acceptable temperature increase on the eyelid. In this optimization study, three parameters were adjusted—the duration of treatment (2, 3, and 4 min), the combinations of cycle numbers in each pulse, and the amplitude of the ultrasound (300/300 mV, 400/400 mV, and 500/500 mV). Temperatures exceeding 41°C were deemed unacceptable due to the risk of thermal injury and would prompt cessation of treatment.<sup>21,22</sup> The final set was chosen as 300/300 mV for a gradual temperature increase around 3 degrees per minute, as shown in Figure 2(e) and (f). The eyelids and ocular surface were inspected during and after treatment to detect thermal injury. The ocular surface was inspected under cobalt blue light after the instillation of fluorescein and topical proparacaine.

### Formal treatment protocol

Six female Dutch belted rabbits were treated under the optimized conditions of 300/300 mV. Three baseline pretreatment measurements were taken on each eye of an awake rabbit. The lipid layer thickness was measured using the LipiView® II ocular interferometer (Figure 1(b) and (c)) (TearScience, Morrisville, NC, USA). The ocular surface was examined with fluorescein staining (BioGlo Fluorescein Sodium Ophthalmic Strips, Jorgensen Laboratories, Inc., Loveland, CO, USA) and photographs taken at the time of the staining. Tear production was measured with Schirmer strips (Merck Animal Health, Kenilworth, NJ, USA).

The rabbit was then anesthetized as mentioned above. The same three measures (LipiView, fluorescein, Schirmer) were repeated. For each rabbit, one eye was randomly chosen to be treated, while the other eye acted as a control. The ultrasound treatment procedure, as described above, was performed for 2 min. The transducer was placed over the closed eyelids and moved over the entire eyelid area to ensure treatment of as many glands as possible. During the treatment, the temperature of the eyelid was recorded every 30 s.

The detailed chosen parameters for the *in vivo* experiment were as follows: the center frequency used for the ultrasound was 3.3 MHz; the pulse repetition frequency (PRF) was 1 kHz; the cycle number was 300 (9% duty cycle); the amplitude of the signal was 300 mV. This combination of cycle number and input voltage was chosen because these conditions induced a temperature increase that was gradual and easy-to-control (~3 degrees per minute). The center frequency was chosen in consideration of the focal area and safety. Lower frequency ultrasound has weaker heating effects in biological tissues; hence, it requires higher acoustic pressure to heat the eyelid. On the other hand, higher frequency ultrasound has a finer heating area with more concentrated energy, making it harder to uniformly heat the whole eyelid.

After the treatments were completed, the transducer, Tegaderm, and thermocouple were removed from the eyelid. The three measurements done prior to treatment (LipiView, fluorescein, Schirmer) were repeated

within 10 min of completion of the procedure. These measurements were again repeated upon awakening from anesthesia, after one week, and after three weeks.

### Lipid layer thickness measurement

The LipiView II ocular interferometer measures lipid layer thickness. The LipiView interferometer captures video of the eye and provides reports based on the videos, which can be analyzed further. A photo of the device and a snapshot of the video are shown in Figure 1(b) and (c). The rabbit eye is blinked manually during LipiView measurements to avoid exposure keratopathy, as the anesthetized rabbit eyelids are open at rest. The interferometer was able to distinguish between an open eye and a closed/blinking eye. Manual blinking was performed for both awake and anesthetized rabbits.

### Fluorescein imaging

One drop of sterile eyewash was placed on a fluorescein strip, and the strip was gently touched to the inferior fornix. The eyelid was manually blinked to disperse the stain. The ocular surface was examined under cobalt blue light without the use of a slit lamp. Therefore, under examination with fluorescein staining, the cornea was noted to be either clear, with evidence of keratopathy, or with frank corneal abrasion.

### Schirmer's test

A Schirmer's test with topical anesthetic was performed as shown in Figure 1(d). The fornices were dried gently, and the Schirmer strip was placed in the inferior fornix. Tear production at 1 min was recorded for each eye.

### Statistical analysis

The Student's paired *t*-test (two-tailed) was performed with MATLAB (R2017a; The MathWorks, Inc., MA, USA) to analyze Schirmer's test results and lipid layer thickness (LLT). Two-way analysis of variance (ANOVA) and Tukey's multiple comparison were also conducted to compare the treatment effects measured at different time points. In all tests,  $p < 0.05$  was considered statistically significant. The results are provided in the form of "mean  $\pm$  standard deviation." Error bars in all figures represent the standard deviation.

## Results

### Ultrasound field and heating effect

The measured ultrasonic spatial-peak-pulse-average intensity was  $I_{SPPA} = 62 \text{ W/cm}^2$ , and the spatial-peak-temporal-average intensity was  $I_{SPTA} = 6.2 \text{ W/cm}^2$ . The mechanical index (MI) was 0.75, which was within the FDA requirement of imaging ultrasound ( $MI < 1.9$ ).

Before the *in vivo* experiment, the ultrasound heating effect was verified and calibrated using gelatin phantoms. Preliminary experiments were then conducted on rabbits to determine a safe temperature and proper treatment time.

Temperature increases in simulation and preliminary experiments are shown in Figure 2(e), comparing the heating effect with different combinations of cycle numbers and input voltages. Figure 2(f) shows the temperature-increasing curves measured in both preliminary experiments and formal experiments, where the parameter combination was 300/300 mV. With increasing treatment times, the eyelid temperature increased. After each ultrasound treatment, the rabbits' eyes were examined for potential injury. Eyelid edema and erythema and exposure keratopathy were observed in the first two preliminary experiments, in which the treatment times were 4 and 3 min, respectively, and temperatures were over 42°C. No injury was observed in the third preliminary experiment in which the treatment time was 2 min. Therefore, to prevent thermal eyelid injury, the treatment time in formal experiments was chosen as 2 min, and the eyelids temperatures were controlled within 41°C. Temperature increasing curves in the formal experiments are shown in Figure 2 by solid lines and points as well. All final temperatures were lower than 41°C.

### The effect of ultrasound treatment

The changes in LLT and tear production were used to evaluate the ultrasound's therapeutic effect on DED, and the results are shown in Figure 3. The change in

values between when the animal was anesthetized and awake are shown in figures as red triangles (anesthetized) and green squares (awake), respectively. Averaged results of both treatment group and control group are shown in Table 1.

An evident increase in LLT with a mean value of 40.33 nm (*paired t test*;  $p < 0.05$ ) was observed after the ultrasound treatment. Meanwhile, the LLT from the control eyes did not show any significant changes. However, during the anesthesia, the mean of LLT slightly decreased from 54.18 nm to 39.00 nm.

The mean values of the Schirmer's test were  $2.0 \pm 2.3$  at pre-treatment (awake) point,  $2.3 \pm 2.9$  at pre-treatment (anesthetized) point,  $4.1 \pm 4.1$  at post-treatment (anesthetized) point, and  $7.2 \pm 4.3$  at post-treatment (awake) point. The overall mean increase in tear flow, measured via Schirmer's test, was 5.2 mm, which is significant enough (*paired T test*;  $p < 0.05$ ) to support the ultrasound treatment effect. In contrast, no significant changes were seen in the control group.

### Examination with fluorescein imaging

Figure 4 shows the representative images of corneal fluorescein staining taken under the cobalt blue light. Examinations of the corneas of all six rabbits in the

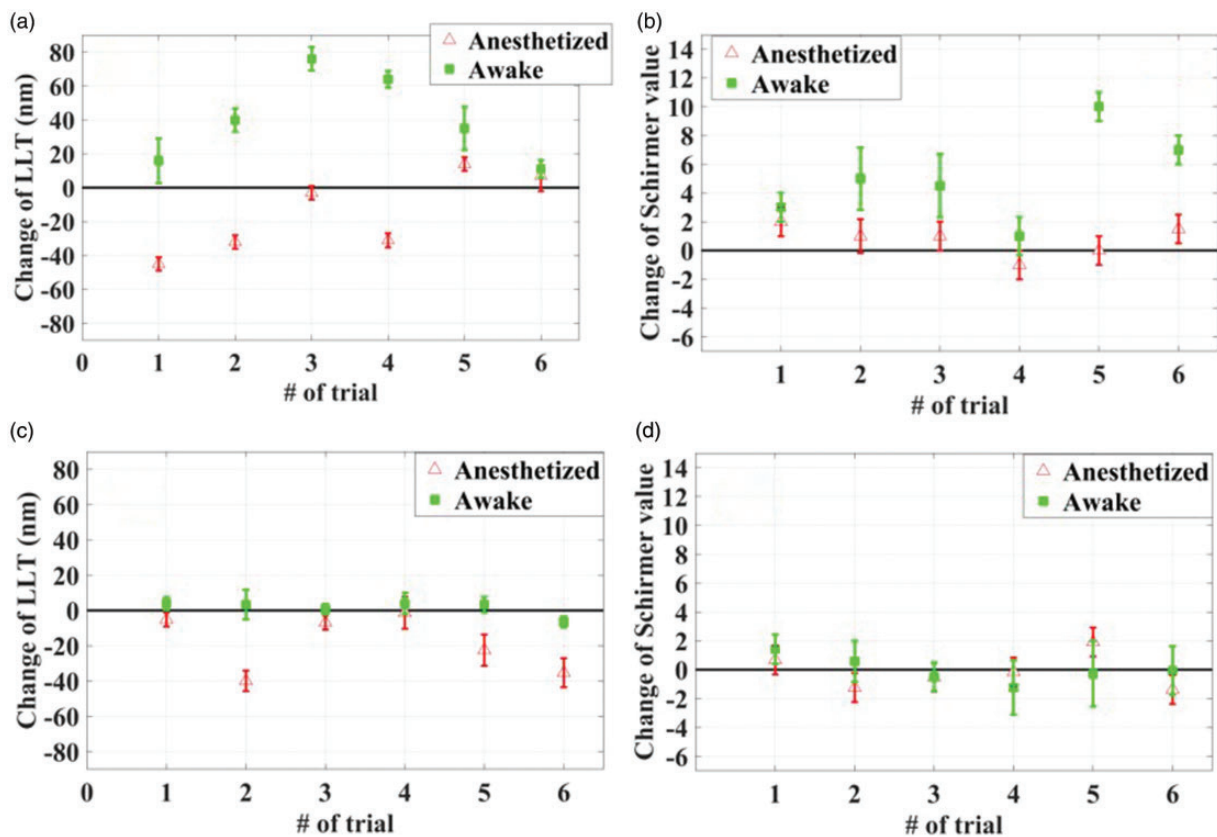


**Figure 3.** Ultrasound treatment effects. (a) and (b) demonstrate the changes of LLT and Schirmer's value before and after the ultrasound treatment. Each trial indicates one rabbit. Red triangles show the changes when the rabbits are anesthetized. Green squares show the changes when the rabbits were awake pre- and post-treatment. (c) and (d) respectively show the changes of LLT and Schirmer's value from the control group. Error bars represent the standard deviation. (A color version of this figure is available in the online journal.)

**Table 1.** Summarized results of LLT and Schirmer's value from all groups.

	Pre-treatment		Post-treatment	
	Awake	Anesthetized	Anesthetized	Awake
Treatment group				
LLT (nm)	55.33 ± 11.15	54.18 ± 13.15	39.00 ± 10.48	95.67 ± 22.77
Schirmer's value	2.0 ± 2.3	2.3 ± 2.9	4.1 ± 4.1	7.2 ± 4.3
Control group				
LLT (nm)	54.79 ± 12.04	53.26 ± 13.95	34.77 ± 10.72	56.29 ± 10.82
Schirmer's value	2.2 ± 1.9	2.1 ± 1.4	2.0 ± 1.8	2.2 ± 1.7

LLT: lipid layer thickness.

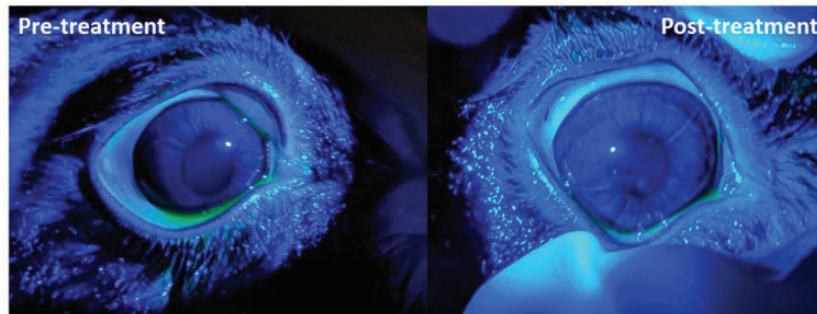


**Figure 4.** Representative images of corneal fluorescein-stained eyes, showing the ocular surfaces' conditions both pre- and post the ultrasound treatment. (A color version of this figure is available in the online journal.)

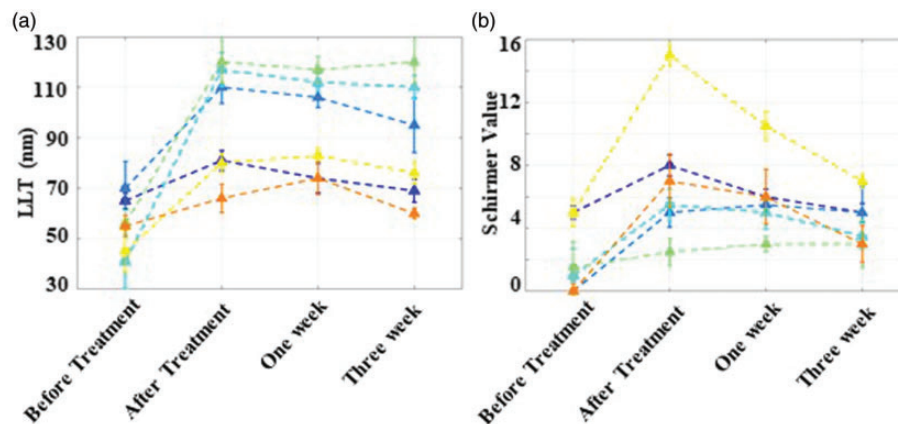


**Figure 5.** Long-term effects of the ultrasound treatment. Measured LLT (a) and Schirmer's values (b) are demonstrated in time sequence. Solid circles are the initial values before the treatment. Triangles show the increased values after the treatment at three time points: right after waking up from anesthesia, one week after the treatment, and three weeks after the treatment. Different rabbits are represented by different colors. Error bars represent the standard deviation. (A color version of this figure is available in the online journal.)

formal experiment were clear without any abrasion pre- and post-treatment.

### Long-term effects

The mean increase in LLT peaked at week 1 (39 nm) but was improved compared to baseline at three weeks after treatment (mean 33 nm, *paired T test*;  $p < 0.05$ ). In contrast, the treatment effect on tear production diminished faster. After one week, the mean increase decreased from 7.2 to 3.9 mm. After three weeks, the mean increase was 2.33 (*paired T test*;  $p < 0.05$ ). Figure 5 shows LLT and Schirmer's testing results before, immediately after, and at one and three weeks after treatment.

### Adverse effects

No long-term adverse effects were observed in all six rabbits used in the formal experiments. In preliminary experiments, there was eyelid erythema, edema, and keratopathy at temperatures greater than 42°C, as noted previously. These symptoms all resolved within one week with the application of topical erythromycin ophthalmic ointment two times per day.

### Discussion

Dry eye is a common and chronic ophthalmic disease that significantly affects patients' quality of life. While no

method currently available can radically cure DED, the proposed ultrasound treatment could be a safe, convenient, and comfortable treatment modality for patients. Considering the shape of the eyelids and the fact that the meibomian glands are distributed medially and laterally throughout the eyelid, the specifically designed line-focused ultrasound transducer reported here is more suitable and efficient than the conventional point-focused transducer.

The safety of any device is of significant concern for a potential ophthalmic treatment procedure. By minimizing the axial resolution (<1.2 mm) and utilizing an ultrasound spacer, the ultrasound treatment area was limited in the eyelids to prevent any direct damage to the ocular surface or eyeball. The fluorescein staining used in this study was an effective method for ocular surface evaluation. Increased corneal staining evident of injury was only observed in the groups that were treated continuously longer than 2 min. The eyelid burns and corneal staining observed in the preliminary study were caused by the local overheating in the eyelids, given that the measured eyelid temperature in these groups was higher than the 42°C.

Two metrics were used in this study to quantify the ultrasound treatment effects. One was Schirmer’s test, which is the classic method for measuring the production of the aqueous component in tears. The other metric was the LLT measured using the commercial device, LipiViewII Interferometer. As it is important for a DED-related study to be able to measure the LLT, LipiView Interferometry provides a non-invasive and useful method for quantifying this metric. In this study, we used the contralateral eyes as controls to avoid errors caused by individual ocular variations and measurement protocols.

Although these rabbits were healthy, we noted the female rabbits’ baseline LLT readings were lower than a couple of the male counterparts that were used early in the process of optimizing the formal testing protocol. We decided to only use female rabbits in the formal testing protocol because lower baseline LLTs would allow for detection of improvement in the LLT in these healthy rabbit models as well as for consistency. This gender discrepancy may be worth exploring in the future should a model for dry eye need to be established for further testing.

It was noted that anesthesia affected the effects of ultrasound treatment. As shown in Figure 6, comparing the LLT of anesthetized animals pre- and post-treatments showed that the LLT slightly decreased to about ~15.18 nm in the treatment group and ~18.49 nm in the control group. Ultrasound cannot be the main reason for the attenuation, since it occurred in both groups. This finding may be due to anesthesia itself impeding or slowing lipid secretion from the meibomian glands while the rabbit is under anesthesia. It has been reported that any condition that results in weakness of the orbicularis muscle will likely have a component of obstructive MGD.<sup>23</sup> Also, the orbicularis oculi would be relaxed during anesthesia.<sup>24,25</sup> Therefore, we infer that the anesthetic phenomenon may be due to the relaxation of orbicularis oculi muscles that help secrete the meibum from the meibomian glands. Once the rabbit was awakened, the full effects of the ultrasound could be appreciated. Similar to the LLT, the increase in tear production was not significant when the animals were still in anesthesia. The effect became evident only after the animals were woken up.

This anesthetic effect would not occur in humans undergoing a similar treatment, as they would not need to be anesthetized for this treatment. This finding is interesting, however, for patients undergoing anesthesia for surgery. One of the reasons that the eye may need to be lubricated during anesthesia is to prevent side effects of dry gritty eyes or even corneal abrasions.

The Schirmer’s increase was somewhat unexpected since the treatment was only specifically targeting the meibomian glands. With the lacrimal gland being on the inferior orbit in rabbits, it is possible that there was some collateral gentle stimulation from the treatment. However, this increase was not as long lasting as the LLT improvement, as shown in Figure 5. Also, in contrast to the relatively stable LLT values, the increase of tear production (Schirmer’s test value) varied significantly among different rabbits, which was reflected by the relatively large standard deviations. Further study, with larger sample size and different genders, would be helpful in better assessing both the effectiveness and safety of the treatment technique.

In conclusion, our results suggest that the ultrasound stimulation on meibomian glands can improve both tear production and lipid secretion. These positive effects can

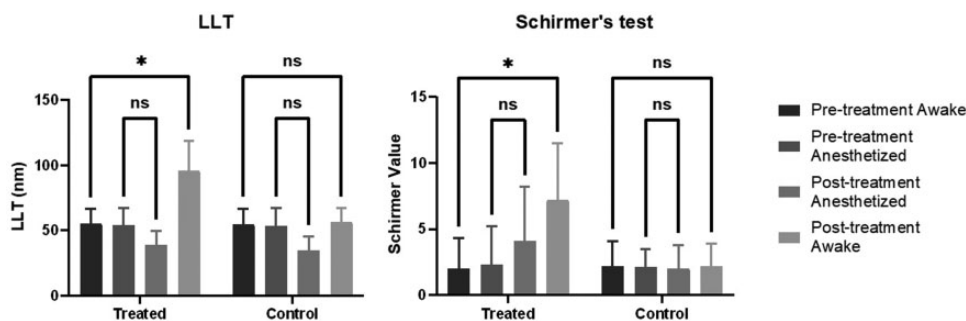


**Figure 6.** Statistical analysis (One-way ANOVA) was conducted to compare the treatment effect at four time points. It is shown that the significant increases were only observed between “Pre-treatment Awake” and “Post-treatment Awake.” “ns” indicates “Not significant,” and “\*” means “ $p < 0.05$ .” Error bars represent the standard deviation.

LLT: lipid layer thickness.

last at least three weeks. No adverse effects were caused by the determined-safe ultrasound treatment settings. With advantages such as safety, convenience, and cost-effectiveness, ultrasound treatment has the potential to become a primary option for patients to treat evaporative DED caused by MGD.

#### AUTHORS' CONTRIBUTIONS

All authors participated in the design, interpretation of the studies, and review of the article; GL, SG, MLP, and SXZ conducted the experiments, GL, RL, and LJ designed and fabricated the ultrasound transducer, and conducted acoustic simulations, GL, SG, PM, and SXZ wrote the article.

#### DECLARATION OF CONFLICTING INTERESTS

The author(s) declared no potential conflicts of interest with respect to the research, authorship, and/or publication of this article.

#### FUNDING

The author(s) disclosed receipt of the following financial support for the research, authorship and/or publication of this article: This work was supported in part by the National Institutes of Health (NIH) under grant (R01EY026091, R01EY028662, R01EY030126, and NIH P30EY029220). SX Zhang-Nunes was also awarded the Zumberge Individual Grant at USC to fund this study. G Lu was awarded the Alfred E. Mann Innovation in Engineering Doctoral Fellowship. An unrestricted departmental grant from Research to Prevent Blindness also supported the study.

#### ORCID iD

Gengxi Lu  <https://orcid.org/0000-0001-7497-050X>

#### REFERENCES

- Group IDEWS. The epidemiology of dry eye disease: report of the epidemiology subcommittee of the international dry eye Workshop (2007). *Ocul Surf* 2007;**5**:93–107
- Lin P-Y, Tsai S-Y, Cheng C-Y, Liu J-H, Chou P, Hsu W-M. Prevalence of dry eye among an elderly Chinese population in Taiwan: the Shihpai eye study. *Ophthalmology* 2003;**110**:1096–101
- Chao W, Belmonte C, del Castillo JMB, Bron AJ, Dua HS, Nichols KK, Novack GD, Schrader S, Willcox MD, Wolffsohn JS. Report of the inaugural meeting of the TFOS i2= initiating innovation series: targeting the unmet need for dry eye treatment. *Ocul Surf* 2016;**14**:264–316
- Schaumberg DA, Sullivan DA, Buring JE, Dana MR. Prevalence of dry eye syndrome among US women. *Am J Ophthalmol* 2003;**136**:318–26
- Schaumberg DA, Dana R, Buring JE, Sullivan DA. Prevalence of dry eye disease among US men: estimates from the physicians' health studies. *Arch Ophthalmol* 2009;**127**:763–8
- Lemp MA, Foulks GN. The definition and classification of dry eye disease. *Ocul Surf* 2007;**5**:75–92
- Foulks G, Lemp M, Jester J, Sutphin J, Murube J, Novack G. Report of the international dry eye workshop (DEWS). *Ocul Surf* 2007;**5**:65–204
- Knop E, Knop N, Millar T, Obata H, Sullivan DA. The international workshop on meibomian gland dysfunction: report of the subcommittee on anatomy, physiology, and pathophysiology of the meibomian gland. *Invest Ophthalmol Vis Sci* 2011;**52**:1938–78
- Baudouin C, Messmer EM, Aragona P, Geerling G, Akova YA, Benítez-del-Castillo J, Boboridis KG, Merayo-Llodes J, Rolando M, Labetoulle M. Revisiting the vicious circle of dry eye disease: a focus on the pathophysiology of meibomian gland dysfunction. *Br J Ophthalmol* 2016;**100**:300–6
- Borchman D, Foulks GN, Yappert MC, Bell J, Wells E, Neravetla S, Greenstone V. Human meibum lipid conformation and thermodynamic changes with meibomian-gland dysfunction. *Invest Ophthalmol Vis Sci* 2011;**52**:3805–17
- Butovich IA, Millar TJ, Ham BM. Understanding and analyzing meibomian lipids – a review. *Curr Eye Res* 2008;**33**:405–20
- Dell SJ. Intense pulsed light for evaporative dry eye disease. *Clin Ophthalmol* 2017;**11**:1167
- Chhadva P, Goldhardt R, Galor A. Meibomian gland disease: the role of gland dysfunction in dry eye disease. *Ophthalmology* 2017;**124**:S20–S26
- Pedrotti E, Bosello F, Fasolo A, Frigo AC, Marchesoni I, Ruggeri A, Marchini G. Transcutaneous periorbital electrical stimulation in the treatment of dry eye. *Br J Ophthalmol* 2017;**101**:814–9
- Villani E, Magnani F, Canton V, Garoli E, Viola F, Ratiglia R. Heating wet chamber goggles (blephasteam®) in meibomian gland dysfunction unresponsive to warm compress treatment. *Investig Ophthalmol Visual Sci* 2012;**53**:602
- del Castillo JMB, Kaercher T, Mansour K, Wylegala E, Dua H. Evaluation of the efficacy, safety, and acceptability of an eyelid warming device for the treatment of meibomian gland dysfunction. *Clin Ophthalmol (Auckland, NZ)* 2014;**8**:2019
- Tufail Y, Yoshihiro A, Pati S, Li MM, Tyler WJ. Ultrasonic neuromodulation by brain stimulation with transcranial ultrasound. *Nat Protoc* 2011;**6**:1453–60
- Lu G, Qian X, Castillo J, Li R, Jiang L, Lu H, Shung KK, Humayun MS, Thomas BB, Zhou Q. Transcranial focused ultrasound for non-invasive neuromodulation of the visual cortex. *IEEE Trans Ultrasonics, Ferroelectrics, Freq Control* 2020;**68**:21–8.
- Zhang Z, Qiu W, Gong H, Li G, Jiang Q, Liang P, Zheng H, Zhang P. Low-intensity ultrasound suppresses low-Mg<sup>2+</sup>-induced epileptiform discharges in juvenile mouse hippocampal slices. *J Neural Eng* 2019;**16**:036006
- Bendau E, Aurup C, Kamimura H, Konofagou E. Low intensity, continuous wave focused ultrasound reversibly depresses heart rate in anesthetized mice. *J Acoust Soc Am* 2019;**146**:2942–43
- Dewhurst M, Viglianti BL, Lora-Michiels M, Hoopes PJ, Hanson MA. Thermal dose requirement for tissue effect: experimental and clinical findings. In: *Thermal treatment of tissue: energy delivery and assessment II: International Society for Optics and Photonics; Proceedings of SPIE the International Society for Optical Engineering*, 2003, vol. 4954, pp.37–57.
- Van Rhoon GC, Samaras T, Yarmolenko PS, Dewhurst MW, Neufeld E, Kuster N. CEM43° C thermal dose thresholds: a potential guide for magnetic resonance radiofrequency exposure levels? *Eur Radiol* 2013;**23**:2215–27
- Allen RC, Wise RJ. Orbicularis oculi weakness and obstructive meibomian gland disease. *JAMA Ophthalmol* 2014;**132**:1490–91
- Altura B, Altura B, Carella A. Effects of ketamine on vascular smooth muscle function. *Br J Pharmacol* 1980;**70**:257
- Lee H, Kim K, Jeong J, Cheong M, Shim J. Comparison of the adductor pollicis, orbicularis oculi, and corrugator supercilii as indicators of adequacy of muscle relaxation for tracheal intubation. *Br J Anaesth* 2009;**102**:869–74

(Received June 23, 2021, Accepted September 10, 2021)